Analysis of cardiopulmonary findings in COVID-19 fatalities: High incidence of pulmonary artery thrombi and acute suppurative bronchopneumonia

Claudia Grosse [a,1,*], Alexandra Grosse [a,1], Helmut J.F. Salzer [b], Martin W. Dünser [c], Reinhard Motz [a], Rupert Langer [a]

[a] *Institute of Pathology and Microbiology, Johannes Kepler University Linz, Altenberger Strasse 69, 4040 Linz, Austria*
[b] *Department of Pulmonology, Kepler University Hospital, Krankenhausstrasse 9, 4041 Linz, Austria*
[c] *Department of Anaesthesiology and Intensive Care Medicine, Kepler University Hospital and Johannes Kepler University Linz, Altenberger Strasse 69, 4040 Linz, Austria*

A R T I C L E I N F O

A B S T R A C T

Since its recognition in December 2019, coronavirus disease 2019 (COVID-19) caused by SARS-CoV-2 has rapidly spread globally causing a pandemic that represents the greatest medical challenge in decades. The aim of the study was to evaluate the spectrum of cardiopulmonary pathology of COVID-19 based on (non-minimal invasive) autopsies performed on 14 COVID-19 decedents. Bilateral diffuse alveolar damage (DAD) was found in all patients. Superimposed acute bronchopneumonia was present in 11 of 14 (78.6%) patients and was considered the major cause of death in 2 patients. A key finding was the presence of thrombotic/thromboembolic vascular occlusions. We classified 5 types of pulmonary thrombi: 1. capillary microthrombi (11/14, 78.6%); 2. partially organized thrombi in mid-sized pulmonary arteries with complete vessel occlusion; 3. non-organized thrombi in mid-sized pulmonary arteries that did not completely fill out the vessel lumen and probably represented thromboemboli rather than thrombosis; 4. bone marrow emboli (1/14, 7.1%); and 5. septic pulmonary thromboemboli (1/14, 7.1%). Pulmonary thrombi in mid-sized arteries were noted in 5 of 14 (35.7%) patients, causing pulmonary infarction and/or pulmonary hemorrhage. All patients had evidence of chronic cardiac disease, including myocardial hypertrophy (13/14, 92.9%), mild to marked coronary artery atherosclerosis (14/14, 100%) and focal myocardial fibrosis (3/14, 21.4%). Acute myocardial infarction was found as concurrent cause of death in 3 (21.4%) patients, and significant cardiac hypertrophy (heart weight 750 g) was present in 1 (7.1%) patient with ATTR-positive cardiac amyloidosis. The autopsy findings confirm that COVID-19 is a systemic disease, with major involvement of the lungs, that increases the risk of cardiac and vascular complications including acute myocardial injury and thrombotic/thromboembolic events. Secondary acute bronchopneumonia is a common complication in patients with COVID-19 and may be the major cause of death.

© 2020 Published by Elsevier Inc.

1. Introduction

Coronavirus disease 2019 (COVID-19) caused by severe acute respiratory coronavirus 2 (SARS-CoV-2) first emerged in December 2019 in Wuhan, China [1,2]. Since then, COVID-19 has spread to at least 188 countries [3] and was officially declared a pandemic by the World Health Organization (WHO) on March 11, 2020 [1,2]. Austria, with its proximity to severely affected Italy and as a major draw for winter sports and après-ski events,

was hit by the pandemic in early March 2020. However, due to strict public safety regulations the number of infections and deaths has been kept comparatively low, with 706 recorded deaths as of July 6, 2020 [3]. Despite relatively low mortality rates a large number of COVID-19 decedents are autopsied in Austria because Austrian law (Section 25 of the Federal Hospitals Act) authorizes pathologists to perform autopsies on deceased patients at public hospitals for the protection of public and scientific interests without formal consent of the next-kind. Most patients with COVID-19 are asymptomatic or have mild symptoms, including fever, dry cough, fatigue and shortness of breath. However, some individuals, especially those with advanced age and

pre-existing comorbidities such as hypertension, diabetes mellitus and cardiovascular disease, develop acute respiratory distress syndrome (ARDS), systemic inflammation and multiorgan dysfunction, associated with high mortality. While previous studies mainly focused on the clinical manifestations, epidemiology and radiographic characteristics of COVID-19, data on the histopathologic findings of COVID-19 are scarce due to barely accessible autopsy or biopsy specimens. Initial reports based on postmortem biopsies have indicated that acute-phase or early organizing-phase diffuse alveolar damage (DAD) is a major histopathologic finding in decedents with COVID-19 pneumonia [4, 5]. Compared with postmortem biopsies or other minimal invasive techniques for tissue sampling, conventional (non-minimal invasive) autopsies offer the advantage of comprehensive tissue sampling, thereby allowing accurate determination of the cause of death and minimizing the risk of sampling error. The aim of the study was to investigate the cardiopulmonary histopathologic findings of COVID-19 based on conventional (non-minimal invasive) autopsies performed on SARS-CoV-2 infected individuals who died during the COVID-19 pandemic. Our findings may help to gain a better understanding of the pathogenic mechanisms underlying cardiopulmonary involvement by SARS-CoV-2. Knowledge of COVID-19 pathology may provide the basis for diagnostic and therapeutic strategies.

2. Materials and Methods

Fourteen consecutive patients with COVID-19 who died at Kepler University Hospital in Linz, Austria, between March 17, 2020, and May 14, 2020, were included in the study. The diagnosis of COVID-19 was confirmed by ante-mortem positive testing for SARS-CoV-2 RNA in nasopharyngeal and oropharyngeal swabs using real-time reverse transcription polymerase chain reaction (RT-PCR). Postmortem external and internal examinations were performed in accordance with recently published biosafety recommendations for autopsies of COVID-19 patients [6]. The deceased were transported from the COVID-19 ward or intensive care unit to the autopsy room in special safety plastic bags. During the autopsy procedure the deceased remained in these plastic bags to reduce contamination. External and internal examination of the body was performed by an experienced pathologist using personal protective equipment including FFP2/3 masks, surgical protection gear, eye protection and 3 layers of gloves, plastic sleeve and two aprons. Tissue samples were collected from the lungs and heart and processed using standard histochemical methods (hematoxylin and eosin staining and additional stains [i.e., Congo red, Prussian blue] where necessary). Elastica van Gieson- and hematoxylin and eosin-stained slides of lung tissue were reviewed on each patient (range, 5 to 15 slides per patient; mean, 10 slides per patient) for the presence or absence of multiple histopathologic features (Table 2). When present, these features were semi-quantitatively assessed by three pathologists in consensus as mild (+), moderate (++) or marked (+++), based on severity of involvement and extent of affected lung tissue. In all patients, representative sections of lung tissue were stained with gram stain, Ziehl Neelsen, periodic acid-Schiff and Grocott methenamine silver stain. Immunohistochemical stainings were performed for CD3, CD20, CD68, thyroid transcription factor (TTF-1) and pancytokeratin using standard protocols. Tissue specimens were also obtained from the liver, spleen, kidneys, intestine and colorectum. Patient demographic characteristics and clinical presentation were recorded. The study was approved by the Ethics Committee of the Medical Faculty of Johannes Kepler University Linz (EK-Nr.78/2020) and conducted in accordance with the regulations issued by the 1964 Helsinki Declaration and its later amendments.

3. Results

3.1. Patient demographic and clinical data

Patient demographic and clinical characteristics are shown in Table 1. The study comprised 9 males and 5 females with a median age of 82 years (range, 55-94 years). Survival duration from symptom onset to death ranged from 6 to 50 days (median, 20 days). The median duration from admission to death was 25 days (range, 2-71 days). The longest disease duration was 50 days in a patient who was tested positive for SARS-CoV-2 RNA throughout a period of 50 days. Seven (50.0%) patients (cases 2, 4, 6, 9, 11, 13 and 14) were admitted to hospital for reasons unrelated to COVID-19 (treatment of dementia: $n = 3$, hip surgery: $n = 1$, dehydration: $n = 1$, treatment for gastric cancer: $n = 1$) and acquired COVID-19 during hospitalization. Seven (50.0%) patients were infected outside the hospital. Presenting symptoms included fever in 11 (78.6%) patients, shortness of breath in 13 (92.9%), fatigue in 10 (71.4%), cough in 7 (50.0%) and diarrhea in 1 (7.1%). One (7.1%) patient died within 36 hours after admission, and 7 (50.0%) patients required intensive care unit support with mechanical ventilation. Each patient had at least one underlying disease. The most common comorbidity was heart disease, including coronary heart disease in 14 (100%), cardiomyopathy in 5 (35.7%), and a history of myocardial infarction in 2 (14.3%). Arterial hypertension was present in 8 (57.1%) patients, neurologic disease including dementia ($n = 5$) and/or a history of cerebral infarction ($n = 2$) in 7 (50.0%), renal disease in 7 (50.0%), diabetes mellitus in 5 (35.7%), malignancy (follicular lymphoma, colorectal cancer, adenocarcinoma of the stomach) in 3 (21.4%), and chronic obstructive pulmonary disease in 6 (42.9%). One (7.1%) patient had a history of deep vein thrombosis. Laboratory test results are summarized in Appendix Table 1. All patients had lymphopenia (lymphocyte count $< 1.0 \times 10^9$/L) on admission or symptom onset in case of hospital-acquired SARS-CoV-2 infection, and all patients had elevated heart enzymes (Troponin T and/or NT-proBNP levels) on preterminal laboratory tests. Fibrinogen (11/14, 78.6%) and D-dimer (14/14, 100%) levels were also frequently elevated. The patients' medications are listed in Appendix Table 2. All patients received anticoagulant and/or antiaggregant therapy, and 10 (71.4%) patients received antibiotic therapy during hospitalization.

3.2. Cardiopulmonary findings

Macroscopically, the lungs were heavy and firm in all patients (390 g to 1340 g for the right lung; 350 g to 1100 g for the left lung), with pronounced pulmonary edema, massive bilateral vascular congestion and patchy to homogeneous dark red to grayish-red appearance of the lung parenchyma in the lower lobes and basal segments of the upper lobes. Two (14.3%) patients had mild serous pleural effusions (50ml/80 ml), and 1 (7.1%) patient had mild fibrinous pleuritis.

The histopathologic findings of lung tissue are summarized in Table 2. All (100%) patients displayed histologic patterns of bilateral DAD. The dominant picture was that of organizing-phase/proliferative DAD, while histologic features of acute-phase/exudative DAD were only mild to moderate. Acute-phase DAD was characterized by hyaline membranes, congestion of alveolar septal capillaries, interstitial edema, mild interstitial lymphocytic inflammation, alveolar exudate and alveolar epithelial desquamation (Figs. 1 and 2A). Organizing DAD was characterized by fibroblastic proliferation within airspaces and alvolar septa, accompanied by mild to moderate interstitial lymphocytic infiltrates that mainly consisted of CD3-positive T-lymphocytes with few scattered CD20-positive B-lymphocytes (Fig. 2B-D). Organizing DAD was frequently associated with type II pneumocyte hyper-

Table 1
Demographic and clinical characteristics of patients with COVID-19.

Case Number	1	2	3	4	5	6	7	8	9	10	11	12	13	14
Gender/Age (years)	M/81	M/71	M/75	W/94	M/55	M/81	M/87	W/83	W/90	W/84	W/80	M/72	M/94	M/82
Symptom onset – death (days)	6	7	10	12	16	17	19	21	21	23	28	29	30	50
Admission – death (days)	2	41	7	24	11	38	9	11	61	22	41	26	71	56
Underlying illness on admission														
Heart disease	Y	Y	Y	Y	Y	Y	Y	Y	Y	Y	Y	Y	Y	Y
Hypertension	N	N	Y	Y	N	Y	Y	Y	N	N	Y	Y	Y	N
Renal disease	Y	N	Y	Y	N	N	N	N	Y	Y	Y	Y	N	Y
Neurologic disease	N	Y	N	Y	N	Y	N	Y	Y	N	Y	N	Y	N
Diabetes mellitus	Y	N	N	N	N	N	N	N	N	Y	Y	Y	N	Y
Malignancy	Y	N	Y	N	N	N	N	N	N	N	N	N	N	Y
Respiratory disease	Y	Y	Y	N	N	N	Y	N	N	N	N	N	Y	Y
Chronic gastritis	N	Y	N	N	N	Y	N	Y	Y	N	Y	Y	N	N
Liver cirrhosis/fibrosis	Y	N	N	N	N	N	N	N	N	N	N	N	N	N
Presenting symptoms														
Fever	Y	Y	Y	Y	Y	Y	N	Y	Y	Y	N	Y	N	Y
Shortness of breath	Y	Y	Y	Y	Y	Y	Y	Y	Y	Y	Y	Y	Y	N
Fatigue	Y	Y	Y	Y	Y	N	Y	Y	N	Y	Y	Y	N	N
Cough	N	N	Y	N	Y	N	Y	Y	Y	N	N	Y	Y	N
Diarrhea	N	N	N	N	N	N	N	N	N	N	N	N	Y	N

Abbreviations: Y, yes; N, no.

Table 2
Histologic features of lung tissue in 14 autopsy cases of COVID-19.

Case Number	1	2	3	4	5	6	7	8	9	10	11	12	13	14	N=14*
Symptom onset – death (days)	6	7	10	12	16	17	19	21	21	23	28	30	30	50	20.7
Total no. of slides	20	20	28	16	23	21	12	16	15	23	17	26	20	25	20.1
No. of slides from the lung	11	11	13	8	11	11	6	7	8	9	10	15	5	8	9.5
Pulmonary capillary congestion	+++	+++	+++	+++	++	++	+++	+++	+++	+++	++	+++	++	++	100.0
DAD, acute	+	+	++	+	+	+	+	+	+	+	++	-	+	-	85.7
Pulmonary edema	+	+++	+	+	+	+	+	+	+	++	+	+	+	++	100.0
DAD, organizing	-	++	++	++	+++	+++	++	+++	++	++	+++	+++	++	++	92.9
Pneumocyte hyperplasia	-	+	++	+	+++	++	++	+++	++	+	+++	++	++	+	92.9
Multinucleated cells	-	-	+	+	+++	++	++	++	+	+	++	++	+	+	85.7
Squamous metaplasia	-	+	++	++	+	+	+	+	+	+	+++	++	+	-	85.7
Acute bronchopneumonia	+++	+++	-	+++	+++	++	-	+	++	++	++	++	+	-	78.6
Pulmonary hemorrhage	+++	++	+	+	+++	++	+	+	+	+	+++	+	+	+	100.0
Infarct	-	-	-	-	+	-	-	-	-	-	+	-	-	-	14.3
Pulmonary microthrombi	-	+	+	-	+	+	-	+	+	+	+	+	+	+	78.6
Thrombi in mid-sized pulmonary arteries	-	+	-	-	+	+	-	-	-	-	+	-	-	+	35.7
Special stains	+	+	-	+	-	+	-	-	-	+	+	+	-	-	50.0

+, mild; ++, moderate; +++, marked; - not present. *Categorical variables are expressed as percentages, numerical variables are expressed as means.
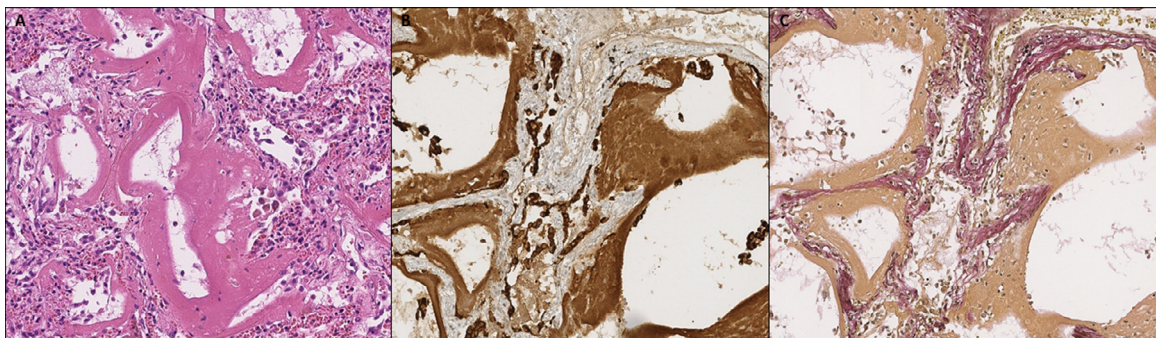
Fig. 1. (A) Acute-phase diffuse alveolar damage with hyaline membranes, highlighted by (B) pancytokeratin and (C) Elastica van Gieson stain.

plasia (13/14, 92.9%) (Fig. 3A), squamous metaplasia (13/14, 92.9%) (Fig. 3B) and multinucleated cells (12/14, 85.7%) that represented either CD68-positive macrophages or pancytokeratin-positive epithelial cells (Fig. 3C,D). No intranuclear or intracytoplasmic viral inclusions were identified at light microscopic examination. Organizing DAD was seen with varying degree and extent in the majority (13/14, 92.9%) of patients. Moderate to marked organizing DAD was the predominant finding in 11 (78.6%) patients with more

than 10 days illness duration. A mixed pattern of coexistent moderate acute- and chronic-phase DAD was present in 1 (7.1%) patient with illness duration of 10 days (Fig. 4A). Two (14.3%) patients with less than 10 days disease duration showed mild and focal acute-phase DAD, one with concomitant minor changes of organizing DAD and both with severe superimposed bacterial bronchopneumonia. Overall, secondary acute bronchopneumonia was seen in 11 of 14 (78.6%) patients, including 2 patients with less than 10 days

Table A1
Laboratory test results of 14 patients with COVID-19.

Case Number	1	2	3	4	5	6	7	8	9	10	11	12	13	14
Blood tests on admission/symptom onset														
Leukocytes ($3.9\text{-}8.8 \times 10^9$/L)	16.81	22.5	2.28	23.83	5.10	11.95	14.38	9.19	5.4	6.79	6.30	9.26	6.49	5.44
Neutrophils ($1.82\text{-}7.42 \times 10^9$/L)	15.65	20.1	2.10	21.04	4.08	11.20	13.83	8.15	4.0	5.52	5.70	7.81	5.20	4.39
Eosinophils ($0.0\text{-}0.5 \times 10^9$/L)	0.0	0.2	0.02	0.05	0.04	0.0	0.00	0.01	0.2	0.0	0.01	0.01	0.0	0.01
Basophils ($0.0\text{-}0.2 \times 10^9$/L)	0.03	0.0	0.0	0.05	0.02	0.02	0.01	0.02	0.0	0.02	0.01	0.03	0.02	0.02
Monocytes ($0.19\text{-}0.77 \times 10^9$/L)	0.97	0.7	0.05	1.95	0.23	1.8	0.17	0.27	0.5	0.51	0.34	0.67	0.46	0.59
Platelets ($151\text{-}400 \times 10^9$/L)	116	295	146	209	271	186	99	223	235	107	164	213	233	93
Lymphocytes ($1.0\text{-}4.0 \times 10^9$/L)	0.16	0.92	0.02	0.74	0.73	0.51	0.32	0.64	0.5	0.74	0.24	0.74	0.81	0.43
CRP (0.0-0.5 mg/dL)	34.6	8.1	10.8	23.5	39.0	19.0	17.5	18.9	0.3	7.7	7.9	17.2	14.7	8.4
Interleukin-6 (0-7 pg/mL)	1133.0	-	80.8	-	220.0	571	-	-	-	34.1	776.0	100.0	35.7	94.1
Fibrinogen (180-400 mg/dL)	>900	331	664	680	>900	640	430	321	635	304	664	675	534	493
D-Dimer (0-0.50 mg/L)	13.10	2.30	5.68	3.21	12.50	2.08	2.28	1.24	7.48	2.21	4.88	3.87	1.31	3.98
Creatinine (0.67-1.17 mg/dL)	3.11	0.68	2.61	1.31	0.81	1.03	1.13	0.83	1.05	1.05	1.42	1.16	0.67	1.88
LDH (135-250 U/L)	620	292	520	863	442	408	640	480	259	371	386	603	290	431
Creatinine kinase (0-190 U/L)	32	188	262	70	53	41	-	-	73	195	67	230	137	21
Troponin T-hs (0.0-14.0 ng/L)	47.4	98	53.8	43.7	7.4	16.5	13.1	8.5	44.5	75.2	69.8	25.0	32.7	12.5
NT-proBNP (0-210 ng/L)	6748	1801	2588	8712	623	830	134	212	2953	8367	4320	408	1463	564
ALAT (10-50 U/L)	16	45	31	87	22	39	40	23	7	24	27	30	22	8
ASAT (10-50 U/L)	48	72	59	98	36	39	25	54	20	98	32	44	52	12
GGT (10-71 U/L)	128	244	29	20	19	31	67	25	10	435	209	125	242	31
ALP (40-129 U/L)	103	136	57	74	36	58	77	34	69	212	163	49	163	44
Amylase (13-53 U/L)	-	-	-	13	-	-	-	-	-	-	-	-	-	-
Lipase (13-60 U/L)	-	-	-	6.1	-	-	-	-	-	-	-	-	-	-
Preterminal blood tests														
Leukocytes ($3.9\text{-}8.8 \times 10^9$/L)	17.59	8.36	1.68	12.82	6.55	7.13	5.45	11.52	4.23	8.36	11.24	11.14	8.4	10.75
Neutrophils ($1.82\text{-}7.42 \times 10^9$/L)	20.80	6.93	1.52	9.23	5.71	6.57	4.80	10.21	2.96	5.04	10.17	7.98	6.0	9.43
Eosinophils ($0.0\text{-}0.5 \times 10^9$/L)	0.0	0.0	0.01	0.0	0.08	0.0	0.02	0.01	0.03	0.12	0.02	0.20	0.2	0.04
Basophils ($0.0\text{-}0.2 \times 10^9$/L)	0.02	0.01	0.0	0.01	0.02	0.04	0.02	0.01	0.02	0.06	0.05	0.05	0.0	0.02
Monocytes ($0.19\text{-}0.77 \times 10^9$/L)	0.78	0.25	0.11	0.41	0.22	0.15	0.13	0.38	0.35	0.62	0.62	0.74	0.5	0.47
Platelets ($151\text{-}400 \times 10^9$/L)	113	244	109	135	119	227	300	415	307	127	205	168	208	111
Lymphocytes ($1.0\text{-}4.0 \times 10^9$/L)	0.14	0.81	0.04	0.96	0.52	0.37	0.45	0.81	0.87	2.52	0.38	2.18	1.7	0.79
CRP (0.0-0.5 mg/dL)	40.3	10.8	39.3	22.4	12.0	32.6	7.2	28.0	2.0	6.4	14.9	23.4	4.1	14.8
Interleukin-6 (0-7 pg/mL)	1246.0	-	438.0	-	13000.0	3018.0	-	-	-	60.7	172.0	407.0	34.4	177.0
Fibrinogen (180-400 mg/dL)	>900	445	>900	844	560	730	>900	535	526	519	833	833	511	571
D-Dimer (0-0.50 mg/L)	12.80	8.50	12.90	4.35	>35.20	10.44	10.21	1.76	3.08	0.95	4.66	1.26	1.40	3.15
Creatinine (0.67-1.17 mg/dL)	3.66	0.73	1.32	1.47	2.35	1.35	0.93	0.57	1.03	1.91	0.59	0.77	0.94	1.83
LDH (135-250 U/L)	635	343	539	349	840	531	713	363	330	447	385	531	233	156
Creatinine kinase (0-190 U/L)	50	292	552	38	796	125	-	-	84	62	19	407	31	23
Troponin T-hs (0.0-14.0 ng/L)	51.0	105.0	60.4	102.0	193.0	105.0	17.3	49	38.6	209.0	119.0	107.0	23.7	36.9
NT-proBNP (0-210 ng/L)	6877	2404	4181	981	1304	4646	187	1345	901	8384	13601	827	1236	1061
ALAT (10-50 U/L)	23	26	24	13	51	41	52	47	18	27	12	37	22	89
ASAT (10-50 U/L)	50	42	72	44	161	67	47	55	38	69	24	94	32	124
GGT (10-71 U/L)	132	201	183	29	49	36	71	56	37	251	109	227	82	2447
ALP (40-129 U/L)	116	148	150	61	71	82	109	67	121	168	184	140	4801	1340
Amylase	-	-	-	-	-	-	-	-	-	-	-	-	-	-
Lipase	-	-	-	-	-	-	-	-	-	-	-	-	-	-

Abbreviations: CRP, C-reactive protein; ALAT, alanine aminotransferase; ASAT, aspartate aminotransferase; ALP, alkaline phosphatase; GGT, glutamyltranspetidase; LDH, lactate dehydrogenase; NT-proBNP, N-terminal fraction of pro-brain natriuretic peptide.

illness duration and 9 of 12 patients with illness duration of 10 days or longer (Fig. 4B,C). The 2 patients with less than 10 days illness duration showed severe acute suppurative bronchopneumonia with dense accumulation of neutrophils within the airways and alveoli, pneumocyte desquamation, vascular congestion and pulmonary hemorrhage. Gram stains revealed gram positive cocci in both cases, and postmortem bacterial cultures from tracheal secretions and lung swabs identified *Staphylococcus aureus* in one case and *Staphylococcus aureus* and *Enterococcus faecalis* in the other. The first case also demonstrated food particles within the airways, indicative of terminal aspiration (Fig. 4D). Among 9 patients with disease duration of 10 days or longer and acute bronchopneumonia, microorganisms were seen on gram stains in 5, including gram positive cocci in 2, gram negative rods in 1, and both gram positive cocci and gram negative rods in 1. One patient showed abundant fungal structures on PAS and Grocott methenamine silver stains. Postmortem cultures were negative for microorganisms in 3 patients and confirmed the presence microorganisms in 6. The most

common pathogen was *Staphylococcus aureus* ($n = 4$), followed by *Klebsiella pneumoniae* ($n = 1$), *Pseudomonas aeruginosa* ($n = 1$) and *Candida sp.* ($n = 1$).

A notable finding was the presence of thrombotic/thromboembolic vascular occlusions in histologic sections of lung tissue. Five types of vascular occlusions could be identified: 1. microthrombi in small alveolar septal arterioles; 2. non-organized fibrinous thrombi in mid-sized pulmonary arteries with partial occlusion of the vessel lumen, likely reflecting pulmonary thromboemboli; 3. partially organized thrombi in mid-sized pulmonary arteries, completely occluding the vessel lumen; 4. bone marrow emboli; and 5. septic pulmonary thromboemboli with evidence of fungal colonization. The most common type of thrombotic/thromboembolic vascular occlusion were capillary microthrombi, present in 11 (78.6%) patients. Thrombi in mid-sized pulmonary arteries were found in 5 (35.7%) patients (Fig. 5A-E). Among those, 1 patient showed partially organized thrombi with complete vessel occlusion, 1 patient showed both

Table A2
Medication of 14 patients with COVID-19.

Medication	1	2	3	4	5	6	7
Anticoagulants	Enoxaparin, 60 mg	Enoxaparin, 40 mg	None	Enoxaparin, 40 mg	Enoxaparin, 40 mg	Enoxaparin, 40 mg	Enoxaparin, 40 mg
Antiplatelet agents	None	None	Acetylsalicylic acid, 100mg	None	None	Acetylsalicylic acid, 100mg	Acetylsalicylic acid, 100mg
Antibiotics	Ampicillin-sulbactam	None	Meropenem	Ampicillin-sulbactam	Clarithromycin, ampicillin-sulbactam	Ampicillin-sulbactam	Piperacillin-tazobactam
Antipyretics	Paracetamol	Paracetamol, metamizole		Paracetamol, metamizole	Paracetamol, metamizole	Paracetamol, metamizole	Paracetamol, metamizole
ACE inhibitors or AT_1-receptor antagonists	None	None	Lisinopril*	None	None	None	None
Other medication	Furosemide, ipratropium-salbutamol, human insulin, digitoxin, pantoprazole, morphine, prothipendyl hydrochloride, haloperidol, diazepam	Furosemide, ipratropium-salbutamol, morphine, lorazepam, pantoprazole	Spironolactone, nebivolol, nicorandil, tiotropiumbro-mid,allopurinol, amlodipine, doxazosin-maleat, pravastatin, pantoprazole, lorazepam, haloperidol	Furosemide, atorvastatin, pantoprazole, allopurinol, digitoxin, pregabalin, metoprolol succinate, alendronate, diazepam	Furosemide, ipratropium-salbutamol, dihydrocodeine hydrohrodanide, hydroxyzine	Furosemide, vitamin D, esomeprazole, lorazepam, simvastatin, valproic acid, trazodone hydrochloride, prothipendyl hydrochloride, pantoprazole	Spironolactone, bisoprolol, amlodipine, ipratropium-salbutamol, L-thyroxine, simvastatin

Medication	8	9	10	11	12	13	14
Anticoagulants	Enoxaparin, 20 mg	Enoxaparin, 40 mg	Enoxaparin, 20 mg	Edoxaban	Enoxaparin, 60 mg	Dabigatran	Dalteparin-natrium
Antiplatelet agents	Acetylsalicylic acid, 100 mg	None	None	None	Acetylsalicylic acid, 100 mg	None	None
Antipyretics	Metamizole	Paracetamol, metamizole	Paracetamol	Paracetamol, prednisolone, azathioprin	Paracetamol	Paracetamol	Paracetamol, metamizole
Antibiotics	Clindamycin	None	Piperacillin-tazobactam	Clindamycin, ampicillin-sulbactam	None	None	Ampicillin-sulbactam
ACE inhibitors or AT_1-receptor antagonists	None	Lisinopril*	None	Candesartan*	Valsartan*	None	None
Other medication	Furosemide, digitoxin, lorazepam, pantoprazole	Furosemide, diazepam, lorazepam, risperidone, haloperidol, pantoprazole	Bisoprolol, amlodipine, digitoxin, rivastigmine, human insulin	Digitoxin, L-thyroxine, furosemide, vitamin D, ropinirole, hydromorphone, gabapentin, pantoprazole, metformin hydrochloride	Furosemide, spironolactone, bisoprolol, fluvastatin, pantoprazole, morphine, vildagliptin-metformin hydrochloride	Furosemide, nicorandil, amlodipine, risperidone, prothipendyl hydrochloride, lorazepam, digitoxin, ipratropium-salbutamol	Furosemide, L-thyroxine, metformin, piritramide, ipratropium-salbutamol

* Received preadmission.

partially organized and non-organized thrombi, and 2 patients showed exclusively non-organized fibrinous thrombi that did not completely fill out the vessel lumen. Bone marrow emboli, likely shock-related, were present in 1 (7.1%) patient with cytokine storm (Fig. 5F), and septic pulmonary thromboemboli with entrapment of neutrophils and fungal structures were identified in 1 (7.1%) patient with a history of deep vein thrombosis. This patient had undergone treatment for gastric cancer before acquiring COVID-19 during hospitalization and had been tested positive for SARS-CoV-2 RNA for a remarkably long period of 50 days prior to his death (Fig. 6). Deep vein thrombosis in the lower extremities was noted in 4 (28.6%) patients, including the patient with septic pulmonary thromboemboli, the 2 patients with exclusively non-organized pulmonary thrombi in mid-sized arteries and the patient with

both partially organized and non-organized pulmonary thrombi in mid-sized arteries. Thrombi were not apparent in the central pulmonary arteries or in any other organs examined, including heart, kidney, liver, spleen and brain. Histopathologic findings associated with thrombotic/thromboembolic vascular occlusions in lung sections included pulmonary infarction, superimposed infection of infarcted lung tissue and pulmonary hemorrhage. Pulmonary hemorrhage, ranging from mild to marked, was seen in all (100%) patients, pulmonary infarction in 2 (14.3%) (Fig. 5G), and secondary infection of the infarcted lung parenchyma in 1 (7.1%) (Fig. 5H).

Cardiovascular and myocardial findings included myocardial hypertrophy (heart weight ranging from 385 g to 750 g) in 13 (92.9%) patients, acute myocardial infarction in 3 (21.4%), focal myocar-
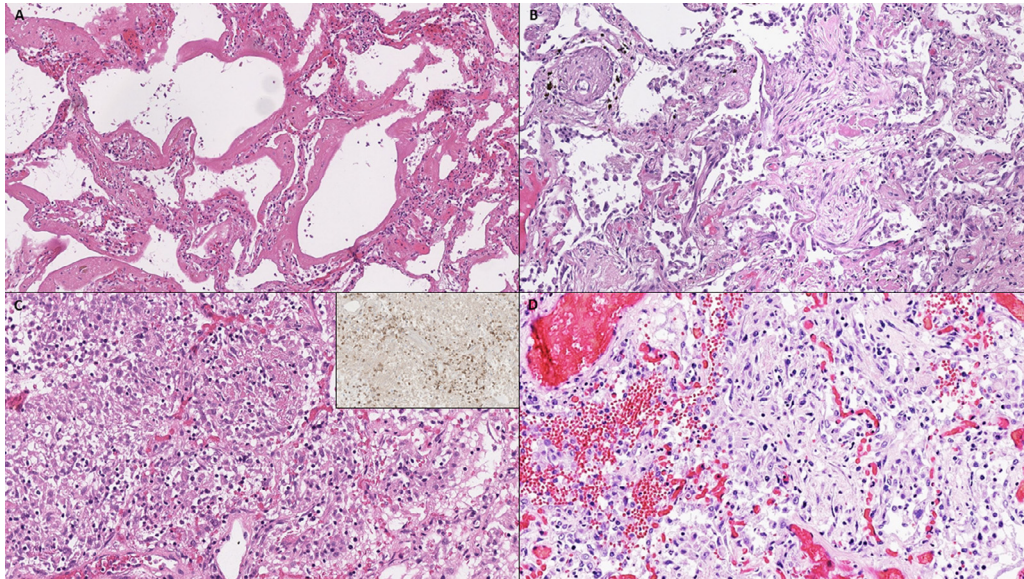
Fig. 2. (A) Acute-phase diffuse alveolar damage with hyaline membranes. (B-D) Chronic-phase diffuse alveolar damage with (B) interstitial and airspace fibroblastic proliferation, (C) lymphocytic infiltrate, mainly composed of CD3-positive T-lymphocytes (inset, CD3), and (D) focal pulmonary hemorrhage.
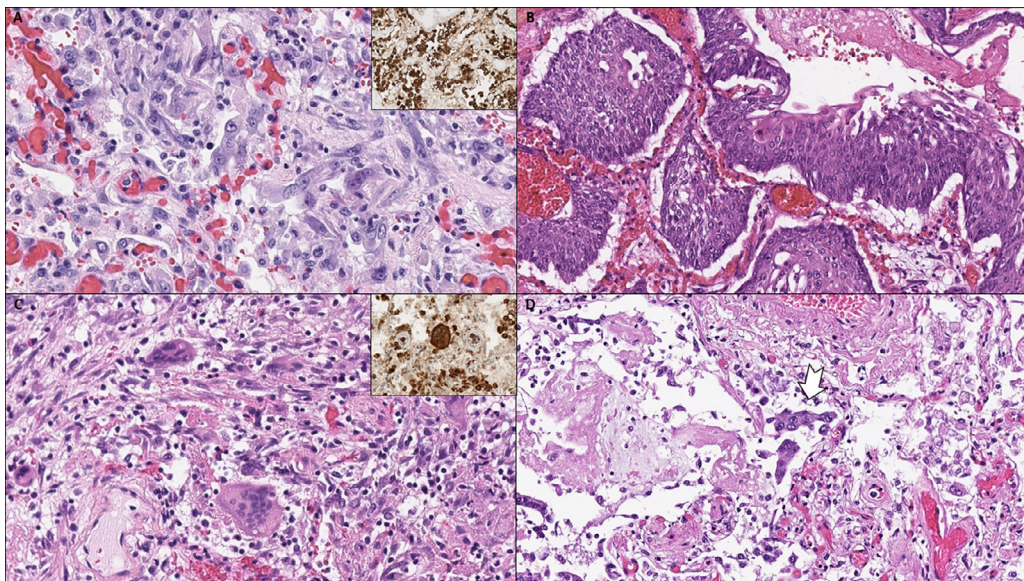
Fig. 3. (A) Hyperplastic type II pneumocytes with some degree of cytological atypia, positive for pancytokeratin showing epithelial lineage of atypical cells (inset). (B) Squamous metaplasia. (C) Multinucleated cells in chronic-phase diffuse alveolar damage, positive for CD68 suggestive of histiocytic cell origin (inset). (D) Syncytical cells of pneumocytic origin (arrow).

dial fibrosis caused by previous myocardial infarction in 6 (42.9%), amyloidogenic transthyretin (ATTR)-positive cardiac amyloidosis in 1 (7.1%), and mild to severe coronary artery atherosclerosis in 14 (100%). Among patients with coronary artery atherosclerosis, 2 had mild 1-vessel coronary artery disease with 25% lumen stenosis, 6 had 2-vessel coronary artery disease (25% lumen stenosis: $n = 1$; 25-50% lumen stenosis: $n = 4$; > 75% lumen stenosis: $n = 1$), and 6 had moderate to severe 3-vessel coronary artery disease (25-50% lumen stenosis: $n = 1$; 50% lumen stenosis: $n = 1$; > 75% lumen stenosis: $n = 4$). All (100%) patients showed at least some mononuclear inflammatory cells in the myocardial interstitium, mainly consisting of CD3-positive T-lymphocytes and ranging in density from average 2 lymphocytes/HPF to 4 lymphocytes/HPF (Fig. 7A).

3.3. Other pathologic findings

Other pathologic findings (Fig. 7B–D), likely related to comorbidities such as arterial hypertension and diabetes mellitus or attributed to shock, included acute renal tubular injury (14/14, 100%), renal arteriolosclerosis (13/14, 92.9%), focal glomerular sclerosis (5/14, 35.7%), mild to moderate liver steatosis (13/14, 92.9%), centrilobular liver congestion (14/14, 100%), mild to moderate portal lymphoid infiltration (12/14, 85.7%), and mild to moderate portal fibrosis (4/14, 28.6%). Specimens from the spleen showed acute splenitis in 2 (14.3%) patients with severe acute bronchopneumonia and moderate white pulp lymphoid depletion in 1 (7.1%) patient with right heart failure and chronic liver and spleen congestion. Histologic examination of intestinal and colorectal mucosa
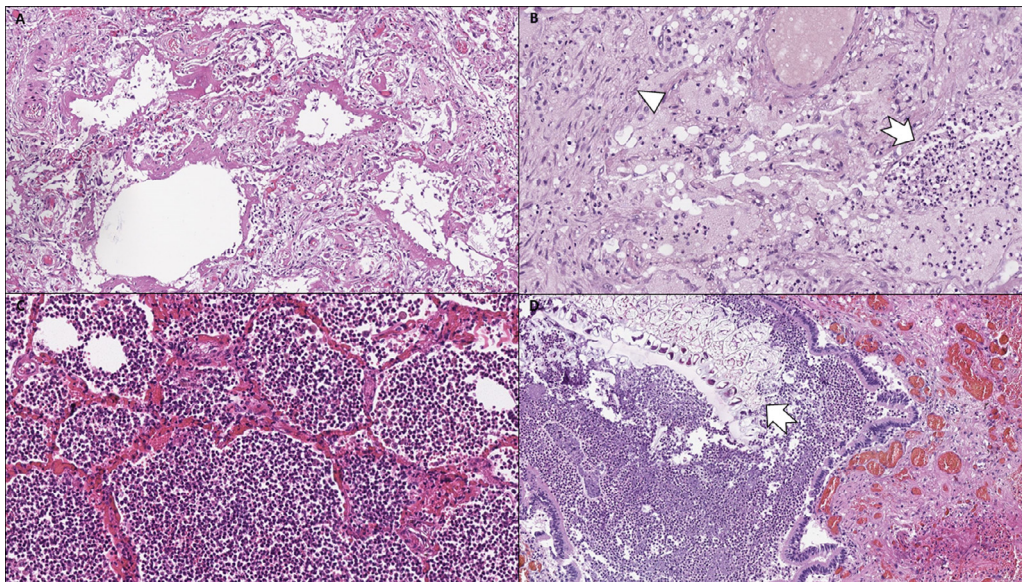
Fig. 4. (A) Interstitial fibroblastic proliferation and hyaline membranes. (B) Organizing diffuse alveolar damage (arrowhead) is seen next to features of acute pneumonia (arrow). (C) Acute bronchopneumonia with dense aggregates of neutrophile granulocytes within the airspaces. (D) A foreign particle (arrow) in a bronchial lumen indicative of terminal aspiration.
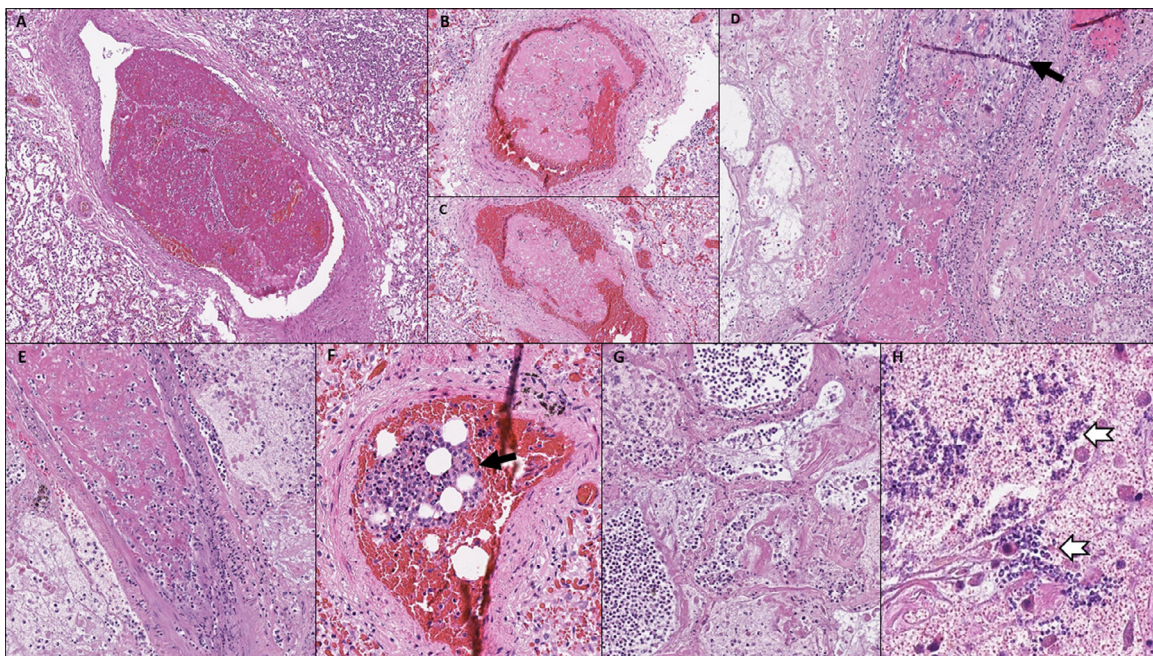
Fig. 5. (A-C) Thrombi in mid-sized pulmonary arteries with incomplete occlusion of the vessel lumen. (D, E) Partially organized thrombi (arrow in D) in mid-sized pulmonary arteries, completely occluding the vessel lumen. (F) Bone marrow embolus. (G) Pulmonary infarction caused by thrombi in mid-sized pulmonary arteries. (H) Fungal superinfection (arrows) in infarcted lung tissue.

was limited by autolysis and showed mild lymphocytic interstitial infiltration in 3 (21.4%) patients. The brain was analyzed in 7 patients and showed atrophy in 4 patients, arteriosclerotic changes in 5, old ischemic infarction in 2, and acute cerebral infarction in 1.

4. Discussion

This paper provides detailed information on the histopathologic spectrum of cardiopulmonary findings of COVID-19 decedents from a major referral center in Austria, Central Europe. We performed conventional (non-minimal invasive) autopsies on 14 deceased pa-

tients with confirmed SARS-CoV-2 infection and systematically investigated the histopathologic cardiopulmonary findings. The main pathologic changes in the lungs consisted of different stages of bilateral DAD. The histopathologic patterns of acute- and chronic-phase DAD were similar to those described in previous studies on COVID-19 pathology [4, 5, 7–12] as well as in autopsy series of patients who died from SARS-CoV-1 during the SARS outbreak in 2002 [13–16]. Although patients with longer disease duration outnumbered those with shorter illness duration in the current study, we were able to show a correlation between histologic patterns of DAD and disease duration, with cases of more than 10 days illness duration showing predominantly organizing DAD and cases
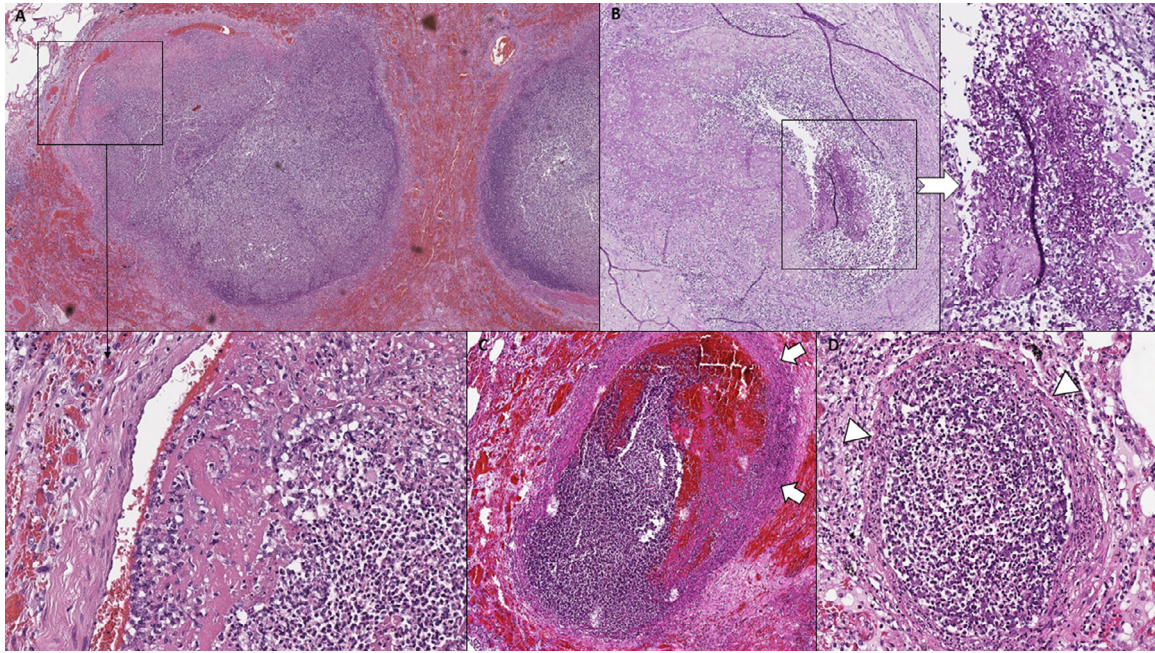
Fig. 6. Pulmonary septicoemboli in a patient with fungal sepsis. (A) Low power magnification shows massively dilated mid-sized pulmonary arteries with intraluminal fibrin deposits and entrapment of neutrophils. (Lower image) High power magnification shows intraluminal fibrin deposits with neutrophilic entrapment and incomplete occlusion of the vessel lumen. (B) Septic embolus consisting of intraluminal fibrin deposits admixed with fungal structures on periodic acid-Schiff stain (right image, high power magnification). (C) Mid-sized pulmonary artery with septic embolus, perivascular hemorrhage and transmural neutrophilic infiltration of the vessel wall (arrows). (D) Septic embolus with transmural neutrophilic infiltration of the vessel wall and involvement of the adjacent lung tissue (arrows).
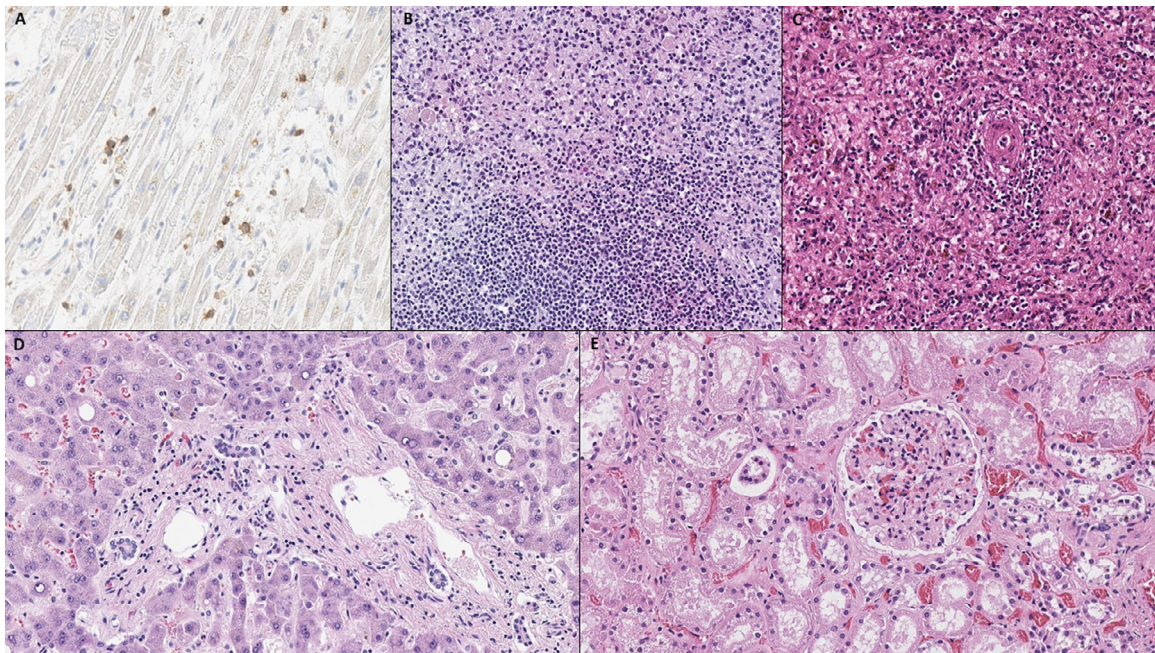
Fig. 7. Extrapulmonary manifestations of COVID-19. (A) Myocardium with few CD3-positive interstitial T-lymphocytes. (B) Spleen with increased neutrophil granulocytes in the perifollicular and marginal zone (splenitis). (C) Spleen with white pulp atrophy. (D) Liver with mild portal lymphocytic infiltration. (E) Kidney with acute tubular damage.

of 10 or fewer days illness duration showing exudative DAD, with or without minor features of organizing DAD. Chronic-phase DAD was commonly associated with squamous metaplasia, type II pneumocyte hyperplasia and multinucleated cells. Squamous metaplasia was seen in the distal bronchioles and alveoli and seems to reflect a reparative response to epithelial lung injury. Hyperplastic pneumocytes may show marked cytological atypia, including enlarged nuclei, cytomegaly, clearing of nuclear chromatin, prominent nucleoli, and multinucleation [13]. The occurrence of multinucleated cells has previously been reported in lung specimens from patients with COVID-19 [4, 5, 8] and SARS-CoV-1 infection [13–16]. While histiocytic multinucleated cells likely represent nonspecific reactive lung changes, it has been proposed that multinucleated epithelial cells could reflect viral-induced cytopathic effect [13–s15]. Yet, the presence of these cells is not unique to SARS-CoV-2, and similar cytological changes can be seen in non-viral cases of DAD and other viral pneumonias like measles, mumps and respiratory syncytial virus [16].

While COVID-19 is known to affect primarily the lungs, it also involves multiple organs, infecting human cells using the angiotensin-converting enzyme-2 (ACE-2) receptor, which is expressed by alveolar epithelium, hepatocytes, biliary epithelium, renal tubular epithelium, enterocytes, and endothelial cells. For pathologists it may be difficult to distinguish COVID-19 related pathologic changes from superimposed infectious processes or underlying illnesses (potentially predisposing to fatal courses). A significant number of patients in our series presented with superimposed acute bronchopneumonia, which could be linked to COVID-19 related lymphopenia, predisposing infected individuals to bacterial or fungal superinfection. Two patients with clinical courses of less than 10 days showed extensive acute suppurative bronchopneumonia with only mild and focal exudative DAD. Because acute bronchopneumonia was the predominant finding in these two cases, we assumed that the patients died from bacterial bronchopneumonia rather than from direct SARS-CoV-2 induced lung injury. Furthermore, all patients in the current study had pre-existing cardiovascular disease and increased NT-proBNP and troponin levels indicative of cardiac injury on preterminal laboratory tests. Studies have shown that in patients with COVID-19 elevated troponin is consistently associated with worse outcomes [17–21], and patients with pre-existing cardiovascular disease are at increased risk of developing complications including myocarditis, acute myocardial infarction, cardiomyopathy, cardiogenic shock, cardiac arrthythmia, and thrombotic or thromboembolic events [22–28]. The mechanisms leading to myocardial injury are not yet completely understood. In the setting of COVID-19, myocardial injury, defined by an elevated troponin level, may be due to unmasking of underlying cardiovascular disease, exacerbated in the setting of physiological stress response, or acute coronary syndrome, triggered by coronary plaque destabilization, demand ischemia or vasospasm in the setting of hemodynamic changes, prothrombotic endothelial dysfunction and exaggerated inflammatory response frequently seen with COVID-19 [17, 18]. Other potential mechanisms of myocardial injury include non-ischemic myocardial processes such as severe respiratory infection with hypoxia, sepsis, systemic inflammation, pulmonary thrombosis and thromboembolism, cardiac adrenergic hyperstimulation during cytokine release syndrome, myocarditis, and stress cardiomyopathy triggered by increased sympathetic stimulation, microcirculatory dysfunction, high catecholamine states, vasospasm and proinflammatory states [17, 18, 28]. In the current study, we found acute myocardial infarction as concurrent cause of death alongside histologically confirmed DAD in 3 patients. One patient presented with a heart weight of 750 g due to massive cardiac amyloidosis (a finding reportedly present in a significant number of COVID-19 decedents [9]). We assumed that this patients died from cardiac decompensation in the context of extensive organizing DAD and pulmonary thrombi, causing pulmonary infarction with superimposed *Candida sp.* pneumonia. Early reports have indicated that fulminant myocarditis may occur in SARS-CoV-2 infection, contributing significantly to morbidity of COVID-19 [29–34]. In addition, acute lymphocytic myocarditis has been demonstrated in endomyocardial biopsies of patients with clinically suspected SARS-CoV-2 associated myocarditis [35, 36]. In the current study, we found only scant T-lymphocytes in the myocardial interstitium on histologic sections of heart tissue. This is consistent with the results of previous autopsy studies [4, 7–9, 11, 37], and we consider this findings of uncertain etiology. We cannot exclude that this observation represents early virus-related inflammatory changes in the myocardium. However, there were no significant lymphocytic inflammatory infiltrates with associated cardiomyocyte damage suggestive of viral myocarditis, and no obvious viral cytopathic effect was observed at light microscopy in the histologic sections of heart tissue; electron microscopic examination was not performed. Further pathologic studies, including ultrastructural analysis, are needed to investigate the effect of SARS-CoV-2 infection on heart vessels and myocardial tissue and to characterize acute myocardial injury in COVID-19 patients. Emerging evidence shows that SARS-CoV-2 infected individuals are at increased risk of thrombotic/thromboembolic events due to a baseline hypercoagulable state. Thrombotic/thromboembolic complications were seen in a significant number of patients in the current series. All patients with pulmonary artery thrombi had elevated D-dimer levels greater than 3.00 mg/L, and the majority of patients had an illness duration of more than 10 days. Based on our histopathologic findings we classified 5 types of pulmonary thrombi. One patient with prolonged clinical course and mild interstitial lung fibrosis showed multiple dilated small to mid-sized pulmonary arteries with intraluminal thrombi infiltrated by numerous neutrophil granulocytes admixed with fungal structures, corresponding to septic pulmonary thromboemboli. Because organizing DAD was only a minor finding in this case, fungal sepsis rather than respiratory failure due to COVID-19 related DAD was considered the cause of death in this patient. Microthrombi in small pulmonary arterioles were a frequent finding, present in 11 (78.6%) patients, and thrombi in mid-sized pulmonary arteries were found in 5 (35.7%) patients. When the vascular lumen was not completely occluded by thrombotic material, we considered this finding to reflect an embolus rather than pulmonary thrombosis. When the affected vessel was completely occluded by partially organized thrombotic material, we assumed that this finding could reflect either pulmonary artery thrombosis or organized pulmonary thromboemboli.

Pulmonary artery thrombi in COVID-19 may be attributed to inflammatory and reparatory mechanisms triggered by alveolar and endothelial damage as a result of DAD. Endothelial damage may be related to host reponse or direct viral infection of endothelial cells, as recently proposed [38]. Furthermore, alvolar fibrin deposition in the event of exudative DAD may affect the delicate local balance of fibrinolysis and coagulation. A combination of alveolar and endothelial damage could lead to microvascular pulmonary thrombosis which then extends to larger-sized pulmonary vessels, contributing to fatal outcomes in SARS-CoV-2 infected individuals [11]. Thrombotic/thromboembolic complications have been reported in autopsy studies of COVID-19 [9–11, 37, 39, 40] as well as in the context of SARS-CoV-1 [13]. In an autopsy series from Singapore, Franks et al. described fibrin thrombi in small pulmonary arteries of 5 of 8 (62.5%) patients with SARS-CoV-1 infection, including 2 of 3 patients with less than 10 days illness duration and 3 of 5 patients with illness duration of 10 days or longer [13]. The authors considered the presence of fibrin thrombi in small pulmonary arteries as common finding of DAD [13]. In the setting of COVID-19, Wichmann et al. reported deep venous thrombosis in 58% and pulmonary microthrombi in 100% of autopsy cases and found pulmonary embolism as the major cause of death in one third of decedents [10]. Lax et al. reported the presence of thrombi in small to mid-sized pulmonary arteries in 100% of COVID-19 autopsy cases as the key pathologic finding [11]. Because the affected pulmonary arteries were completely occluded by thrombotic material, the authors considered their findings to reflect pulmonary thrombosis rather than pulmonary thromboembolism. In another autopsy series, Menter et al. described pulmonary microthrombi in 45%, pulmonary embolism in 19% and fibrin thrombi in glomerular capillaries in 18% of COVID-19 autopsy cases [9]. As the authors suggested, the frequent findings of pulmonary capillarostasis and microthrombi in the lungs and kidneys could imply an impaired microcirculation. Hence, COVID-19 related coagulopathy, with features of both disseminated intravascular coagulation and thrombotic microangiopathy, may play an important role in disease progression and lethality [9].

5. Conclusion

Our study shows that secondary acute bronchopneumonia can be found in a substantial number of patients with COVID-19 and may be the major cause of death. Furthermore, a high incidence of thrombotic/thromboembolic events is seen in COVID-19 decedents. We classified 5 types of thrombotic/thromboembolic vascular occlusions in lung specimens from COVID-19 decedents: microthrombi; non-organized thrombi in mid-sized pulmonary arteries with incomplete occlusion of the vessel lumen, likely representing pulmonary thromboemboli; partially organized thrombi in mid-sized pulmonary arteries completely occluding the vessel lumen; bone marrow emboli, likely shock-related; and septic pulmonary thromboemboli. Our findings support the concept that COVID-19 is a systemic disease, with major involvement of the lungs, that increases the risk of thrombotic/thromboembolic events and cardiac complications, contributing to fatal outcomes in SARS-CoV-2 infected individuals.

Funding

Availability of data and materials

The datasets supporting the conclusions of this article are available from the corresponding author on reasonable request.

Author's contributions

CG, AG, and RL were responsible for the conceptualization of this study and the project administration. CG, AG, HS, MD and RM were responsible for data collection and literature analysis. AG and CG were responsible for analysis and data interpretation. CG and AG wrote the manuscript. All authors critically revised the manuscript and approved the final version.

Ethics approval and consent to participate

The study was approved by the Ethics Committee of the Medical Faculty of Johannes Kepler University Linz (EK-Nr. 78/2020).

Declaration of competing interest

The authors declare that they have no competing interests.

Acknowledgements

References

[1] Park SE. Epidemiology, virology, and clinical features of severe acute respiratory syndrome-coronavirus-2 (SARS-CoV-2; Coronavirus Disease-19). Clin Exp Pediatr 2020;63:119–24. doi:10.3345/cep.2020.00493.

[2] Lu H, Stratton CW, Tang YW. Outbreak of pneumonia of unknown etiology in Wuhan, China: The mystery and the miracle. J Med Virol 2020;92:401–2. doi:10.1002/jmv.25678.

[3] Johns Hopkins University&Medicine. COVID-19 dashboard by the Center for Systems Science and Engineering (CSSE). Available at: https://coronavirus.jhu.edu/map.html; Accessed July 6, 2020.

[4] Xu Z, Shi L, Wang Y, Zhang J, Huang L, Zhang C, et al. Pathological findings of COVID-19 associated with acute respiratory distress syndrome. Lancet Respir Med 2020;8:420–2. doi:10.1016/S2213-2600(20)30076-X.

[5] Tian S, Xiong Y, Liu H, Niu L, Guo J, Liao M, et al. Pathological study of the 2019 novel coronavirus disease (COVID-19) through postmortem core biopsies. Mod Pathol 2020. doi:10.1038/s41379-020-0536-x.

[6] Hanley B, Lucas SB, Youd E, Swift B, Osborn M. Autopsy in suspected COVID-19 cases. J Clin Pathol 2020;73:239–42. doi:10.1136/jclinpath-2020-206522.

[7] Duarte-Neto AN, de Almeida Monteiro RA, Ferraz da Silva LF, et al. Pulmonary and systemic involvement of COVID-19 assessed by ultrasound-guided minimally invasive autopsy. Histopathology 2020. doi:10.1111/his.14160.

[8] Barton LM, Duval EJ, Stroberg E, Ghosh S, Mukhopadhyay S. COVID-19 autopsies, Oklahoma, USA. Am J Clin Pathol 2020. doi:10.1093/ajcp/aqaa062.

[9] Menter T, Haslbauer JD, Nienhold R, Savic S, Hopfer H, Deigendesch N, et al. Post-mortem examination of COVID19 patients reveals diffuse alveolar damage with severe capillary congestion and variegated findings of lungs and other organs suggesting vascular dysfunction. Histopathology 2020. doi:10.1111/his.14134.

[10] Wichmann D, Sperhake JP, Lütgehetmann M, Steurer S, Edler C, Heinemann A, et al. Autopsy findings and venous thromboembolism in patients with COVID-19: a prospective cohort study. Ann Intern Med 2020. doi:10.7326/M20-2003.

[11] Lax SF, Skok K, Zechner P, Kessler HH, Kaufmann N, Koelblinger C, et al. Pulmonary arterial thrombosis in COVID-19 with fatal outcome: results from a prospective, single-center, clinicopathologic case series. Ann Int Med 2020. doi:10.7326/M20-2566.

[12] Tian S, Hu W, Niu L, et al. Pulmonary pathology of early-phase 2019 novel coronavirus (COVID-19) pneumonia in two patients with lung cancer. J Thorac Oncol 2020. doi:10.1016/j.jtho.2020.02.010.

[13] Franks TJ, Chong PY, Chui P, Galvin JR, Lourens RM, Reid AH, et al. Lung pathology of severe acute respiratory syndrome (SARS): a study of 8 autopsy cases from Singapore. Hum Pathol 2003;34:743–8. doi:10.1016/s0046-8177(03)00367-8.

[14] Nicholls JM, Poon LL, Lee KC, Ng WF, Lai ST, Leung CY, et al. Lung pathology of fatal severe acute respiratory syndrome. Lancet 2003;361:1773–8. doi:10.1016/s0140-6736(03)13413-7.

[15] Ksiazek TG, Erdman D, Goldsmith CS, Zaki SR, Peret T, Emery S, et al. A novel coronavirus associated with severe acute respiratory syndrome. N Engl J Med 2003;348:1953–66. doi:10.1056/NEJMoa030781.

[16] Tse G M-K, To K-F, Chan P K-S, Lo AWI, Ng K-C, Wu A, et al. Pulmonary pathological features in coronavirus associated severe acute respiratory syndrome (SARS). J Clin Pathol 2004;57:260–5. doi:10.1136/jcp.2003.013276.

[17] Imazio M, Klingel K, Kindermann I, Brucato A, De Rosa FG, Adler Y, et al. COVID-19 pandemic and troponin: indirect myocardial injury, myocardial inflammation or myocarditis? Heart 2020 heartjnl-2020-317186. doi:10.1136/heartjnl-2020-317186.

[18] Cheng R, Leedy D. COVID-19 and acute myocardial injury: the heart of the matter or an innocent bystander? Heart 2020. doi:10.1136/heartjnl-2020-317025.

[19] Wei J, Huang F, Xiong T, et al. Acute myocardial injury is common in patients with COVID-19 and impairs their prognosis. Heart 2020;106:1155–60.

[20] Guo T, Fan Y, Chen M, Wu X, Zhang L, He T, et al. Cardiovascular implications of fatal outcomes of patients with coronavirus disease 2019 (COVID-19). JAMA Cardiol 2020. doi:10.1001/jamacardio.2020.1017.

[21] Shi S, Qin M, Shen B, Cai Y, Liu T, Yang F, et al. Association of cardiac injury with mortality in hospitalized patients with COVID-19 in Wuhan, China. JAMA Cardiol 2020. doi:10.1001/jamacardio.2020.0950.

[22] Kang Y, Chen T, Mui D, Ferrari V, Jagasia D, Scherrer-Crosbie M, et al. Cardiovascular manifestations and treatment considerations in covid-19. Heart 2020. doi:10.1136/heartjnl-2020-317056.

[23] Guzik TJ, Mohiddin SA, Dimarco A, Patel V, Savvatis K, Marelli-Berg FM, et al. COVID-19 and the cardiovascular system: implications for risk assessment, diagnosis, and treatment options. Cardiovasc Res 2020. doi:10.1093/cvr/cvaa106.

[24] Long B, Brady WJ, Koyfman A, Gottlieb M. Cardiovascular complications in COVID-19. Am J Emerg Med 2020. doi:10.1016/j.ajem.2020.04.048.

[25] Li JW, Han TW, Woodward M, Anderson CS, Zhou H, Chen YD, et al. The impact of 2019 novel coronavirus on heart injury: a systemic review and meta-analysis. Prog Cardiovasc Dis 2020. doi:10.1016/j.pcad.2020.04.008.

[26] Hendren NS, Drazner MH, Bozkurt B, Cooper LT. Description and proposed management of the acute COVID-19 cardiovascular syndrome. Circulation 2020. doi:10.1161/CIRCULATIONAHA.120.047349.

[27] Kochi AN, Tagliari AP, Forleo GB, Fassini GM, Tondo C. Cardiac and arrhythmic complications in patients with COVID-19. J Cardiovasc Electrophysiol 2020. doi:10.1111/jce.14479.

[28] Babapoor-Farrokhran S, Gill D, Walker J, Rasekhi RT, Bozorgnia B, Amanullah A. Myocardial injury and COVID-19: possible mechanisms. Life Sci 2020;253:117723. doi:10.1016/j.lfs.2020.117723.

[29] Zeng JH, Liu YX, Yuan J, Wang FX, Wu WB, Li JX, et al. First case of COVID-19 complicated with fulminant myocarditis: a case report and insights. Infection 2020:1–5. doi:10.1007/s15010-020-01424-5.

[30] Paul JF, Charles P, Richaud C, Caussin C, Diakov C. Myocarditis revealing COVID-19 infection in a young patient. Eur Heart J Cardiovasc Imaging 2020;21:776. doi:10.1093/ehjci/jeaa107.

[31] Beşler MS, Arslan H. Acute myocarditis associated with COVID-19 infection. Am J Emerg Med 2020;S0735-6757(20):30460–3. doi:10.1016/j.ajem.2020.05.100.

[32] Joob B, Wiwanitkit V. Fulminant myocarditis and COVID-19. Rev Esp Cardiol (Engl Ed) 2020;S1885-5857(20):30203–6. doi:10.1016/j.rec.2020.05.006.

[33] Kim I-C, Kim JY, Kim HA, Han S. COVID-19-related myocarditis in a 21-year-old female patient. Eur Heart J 2020;41:1859. doi:10.1093/eurheartj/ehaa288.

[34] Hu H, Ma F, Wei X, Fang Y. Coronavirus fulminant myocarditis saved with glucocorticoid and human immunoglobulin. Eur Heart J 2020. doi:10.1093/eurheartj/ehaa190.

[35] Sala S, Peretto G, Gramegna M, Palmisano A, Villatore A, Vignale D, et al. Acute myocarditis presenting as a reverse Tako-Tsubo syndrome in a patient with SARS-CoV-2 respiratory infection. Eur Heart J 2020;41:1861–2. doi:10.1093/eurheartj/ehaa286.

[36] Tavazzi G, Pellegrini C, Maurelli M, Belliato M, Sciutti F, Bottazzi A, et al. Myocardial localization of coronavirus in COVID-19 cardiogenic shock. Eur J Heart Fail 2020;22:911–15. doi:10.1002/ejhf.1828.

[37] Fox SE, Akmatbekov A, Harbert JL, Li G, Brown JQ, Vander Heide RS. Pulmonary and cardiac pathology in African American patients with COVID-19: an autopsy series from New Orleans. Lancet Respir Med 2020;8:681–6. doi:10.1016/S2213-2600(20)30243-5.

[38] Varga Z, Flammer AJ, Steiger P, Haberecker M, Andermatt R, Zinkernagel AS, et al. Endothelial cell infection and endotheliitis in COVID-19 [Letter]. Lancet 2020;395:1417–18.

[39] Buja LM, Wolf DA, Zhao B, Akkanti B, McDonald M, Lelenwa L, et al. The emerging spectrum of cardiopulmonary pathology of the coronavirus disease 2019 (COVID-19): report of 3 autopsies from Houston, Texas, and review of autopsy findings from other United States cities. Cardiovasc Pathol 2020;48:107233. doi:10.1016/j.carpath.2020.107233.

[40] Grimes Z, Bryce C, Sordillo EM, Gordon RE, Reidy J, Paniz Mondolfi AE, et al. Fatal pulmonary thromboembolism in SARS-CoV-2-infection. Cardiovasc Pathol 2020;48:107227. doi:10.1016/j.carpath.2020.107227.